Journal of Medicinal Chemistry

Article

Design and Synthesis of Dual-action Inhibitors Targeting Histone Deacetylases and HMG-CoA Reductase for Cancer Treatment

Jhih-Bin Chen, Ting-Rong Chern, Tzu-Tang Wei, Ching-Chow Chen, Jung-Hsin Lin, and Jim-Min Fang

J. Med. Chem., **Just Accepted Manuscript** • DOI: 10.1021/jm400179b • Publication Date (Web): 09 Apr 2013

Just Accepted

ACS Publications
High quality. High impact.

Journal of Medicinal Chemistry is published by the American Chemical Society.
1155 Sixteenth Street N.W., Washington, DC 20036

Design and Synthesis of Dual-action Inhibitors Targeting Histone Deacetylases and HMG-CoA Reductase for Cancer Treatment

Jhih-Bin Chen,[†,#] Ting-Rong Chern,[‡,#] Tzu-Tang Wei,[¶,#] Ching-Chow Chen,[¶] Jung-Hsin Lin,*[,‡] and Jim-Min Fang*[,†]

[†]Department of Chemistry, National Taiwan University, Taipei 106, Taiwan.

[‡]School of Pharmacy, National Taiwan University, Taipei 100, Taiwan.

[¶]Department of Pharmacology, College of Medicine, National Taiwan University, Taipei 100, Taiwan.

[#]These authors contributed equally to this work.

ABSTRACT

A series of dual-action compounds were designed to target histone deacetylase (HDAC) and 3-hydroxy-3-methylglutaryl coenzyme A reductase (HMGR) by having a hydroxamate group essential for chelation with the zinc ion in the active site of HDAC and the key structural elements of statin for binding with both proteins. In our study, the statin hydroxamic acids prepared by fused strategy are most promising in cancer treatments. These compounds showed potent inhibitory activities against HDACs and HMGR with IC_{50} values in nanomolar range. These compounds also effectively reduced the HMGR activity as well as promoted the acetylations of histone and tubulin in cancer cells, but were not toxic to normal cells.

INTRODUCTION

Cancer cells may be developed from inherited defects or acquired damages of DNA. Cancer is a highly complex multi-genetic disease involving multiple cross-talks between signaling networks. Using drug-cocktails that combine multiple anti-cancer agents working in different mechanisms has been a standard treatment of cancers to avoid drug resistance.[1–4]

Histone acetyltransferases (HATs) and histone deacetylases (HDACs) have recently emerged as important targets for cancer therapy. Acetylation of the lysine residues on histone H3 and H4 leads to a loose and active chromatin, which allows access of various transcription factors to the promoters of target genes. In contrast, deacetylation of the lysine residues results in a highly compact and transcriptionally inactive chromatin.[5] The levels of histone acetylation and deacetylation are regulated by HATs and HDACs, respectively.[6] HDAC overexpression has been found in a variety of human cancers, including myeloid neoplasia and solid tumors.[7] The association of HDACs with oncogenic DNA-binding fusion proteins and other repressive transcription factors constitutively suppresses specific tumor suppressor genes.[8] Therefore, HDACs represent a rational target for cancer treatment. Several HDAC inhibitors (HDACi's) are currently under clinical trials on either monotherapy or combination therapy for cancer treatment.[9, 10] HDACi's are categorized into four groups: short-chain fatty acids, hydroxamic acids, cyclic tetrapeptides, and benzamides.[8] Among them, the hydroxamate-containing HDACi's trichostatin A (TSA) and suberoylanilide hydroxamic acid

(SAHA, Figure 1A) exhibit the most potent efficacy.

In another aspect, statins have recently been shown to be effective for cancer prevention in observational, preclinical, and certain randomized controlled studies.[11] Statins, such as lovastatin (Figure 1B) and atorvastatin, are known to reduce serum cholesterol levels through competitive inhibition at 3-hydroxy-3-methylglutaryl coenzyme A reductase (HMGR). The HMGR inhibitors (HMGRi's) are effectively used to decrease the incidence of cardiovascular and cerebrovascular disorders, and to prevent cardiovascular disease (CVD).[12] Statins possess an established record of safety and efficacy in human CVD prevention.

It has been reported that the combination use of anticancer agents with statins may reduce side effects to attain better treatment of cancers.[13] Furthermore, the *in vitro* experiment using combination of HDACi and HMGRi has shown the synergistic induction of apoptosis of HeLa cells.[15] The underlying synergistic mechanism has been proposed that the down-regulation of geranylgeranyltransferase (GGTase)-I β subunit, caused by HDACi (TSA in that study), enhances the depletion of mevastatin-induced geranylgeranylated RhoA.[14] However, the direct HDAC inhibition by statins[15] could have also made significant contributions to this synergism.

Given the aforementioned evidence, we conceived that concurrent inhibition of HDAC and HMGR would be a promising approach for cancer treatment. However, using multi-component drug-cocktails for therapeutics has some drawbacks, such as complex

pharmacokinetics, unpredictable drug–drug interaction, and formulation problems due to different solubilities of individual drugs.[16, 17] Alternatively, to design a single compound that simultaneously modulates multiple targets, dubbed designed multiple ligand (DML), has become an emerging paradigm for drug discovery.[16, 18] DMLs constructed by incorporation of HDACi's into other active agents targeting inosine monophosphate dehydrogenase,[19, 20] nuclear vitamin D receptor,[21] tyrosine kinase receptor[22, 23] or topoisomerase II[24] have been tested in cancer treatments.[25]

In this study, we designed the dual-action anticancer agents **6a**, **6b**, **10**, and **12**–**15** by the knowledge- and structure-based approaches to target both HDAC and HMGR (Figure 1C–E).[17, 26] The rationale for the dual-inhibitor design was originated from our previous modeling work,[16] which showed that lovastatin could fit the adjacent transient pocket about 4 Å away from the active site of HDAC. We first designed the HMGR–HDAC dual inhibitors **6a**,**b** by direct connection of lovastatin with a triazole-linked SAHA[27] (Figure 1C). According to the structural information,[28] the hydroxamate group plays an essential role in chelation of zinc ion for HDAC inhibition, whereas the hydrophobic moiety of SAHA can be replaced by lovastatin fragment to accommodate with the deep pocket of HDAC. In the meantime, compounds **6a**,**b** still retain the HMG-like structure to assure their potency to HMGR.[29] These conjugated molecules were predicted to hold the key interactions with the two enzymes to exert the desired biological functions. To reduce the molecular weight of dual inhibitor, we

further prepared a merged molecule **10** (Figure 1D), in which the two essential pharmacophoric elements, hydroxamic acid and hydrophobic moiety, are linked by a short aliphatic chain. We finally realized that the aliphatic chains in SAHA and lovastatin could be overlaid (Figure 1E), so that the fused molecules could act as HMGR–HDAC dual-targeting inhibitors. We report herein the synthesis, molecular modeling and biological activities of these conjugated, merged and hybrid HMGR–HDAC inhibitors.

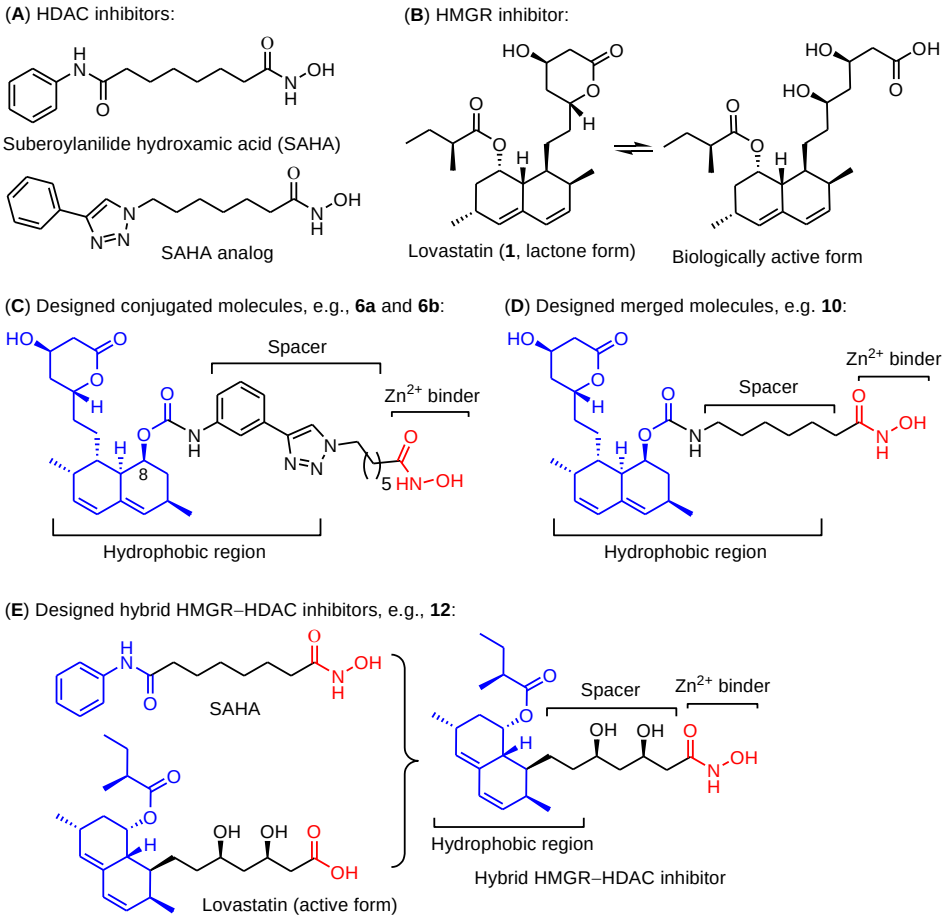

Figure 1. Designed dual inhibitors for HMG-CoA reductase (HMGR) and histone deacetylase (HDAC). (**A**) Structure of a representative HMGR inhibitor. (**B**) Structures of representative

HDAC inhibitors. (**C**) Design of lovastatin derivative bearing hydroxamic acid group by conjugation strategy via click reaction. (**D**) Design of lovastatin derivative bearing hydroxamic acid group by merged strategy using a short aliphatic spacer. (**E**) Design of lovastatin hydroxamic acid by fused strategy to share a common 6-carbon unit from SAHA and lovastatin. The hydroxamic acid (red) is a surrogate of the carboxylate group in lovastatin, and acts as a zinc chelation group for HDAC inhibition. The HMG-like moiety (blue) provides the appropriate interactions with HMGR and HDAC.

RESULTS AND DISCUSSION

Chemistry. To synthesize the conjugated compounds **6a**,**b** (Scheme 1), lovastatin in the lactone form was treated with KOH in H_2O/MeOH to open the lactone ring and to cleave the ester bond. The lactone ring was regenerated by treatment with HCl (6 M) for 4.5 h at room temperature without causing side reactions due to elimination of water molecules. A bulky tetrabutyldimethylsilyl (TBS) group was selectively introduced to protect the less hindered hydroxyl group, giving intermediate **2**. The subsequent treatment of **2** with *p*-nitrophenyl chloroformate in the presence of pyridine and 4-dimethylaminopyridine (DMAP) afforded the carbonate **3**. The substitution reactions of **3** with 4-ethynylaniline and 4-ethynylbenzylamine were carried out to provide the carbamates **4a** and **4b** in 66% and 90% yields, respectively. Compounds **4a** and **4b** were then subjected to the Cu^+-catalyzed 1,3-dipolar cycloadditions

(click reactions) with 7-azidoheptanoic acid to give practically pure triazole products **5a** and **5b**, which were isolated simply by extraction with EtOAc. The acids **5a** and **5b** were activated by treatment with ethyl chloroformate to form mixed anhydrides, which were reacted *in situ* with hydroxylamine to give hydroxamates **6a** and **6b** in modest yields.

Scheme 1. Synthesis of lovastatin derivatives **6a** and **6b** bearing hydroxamic acid group by conjugation strategy.[a]

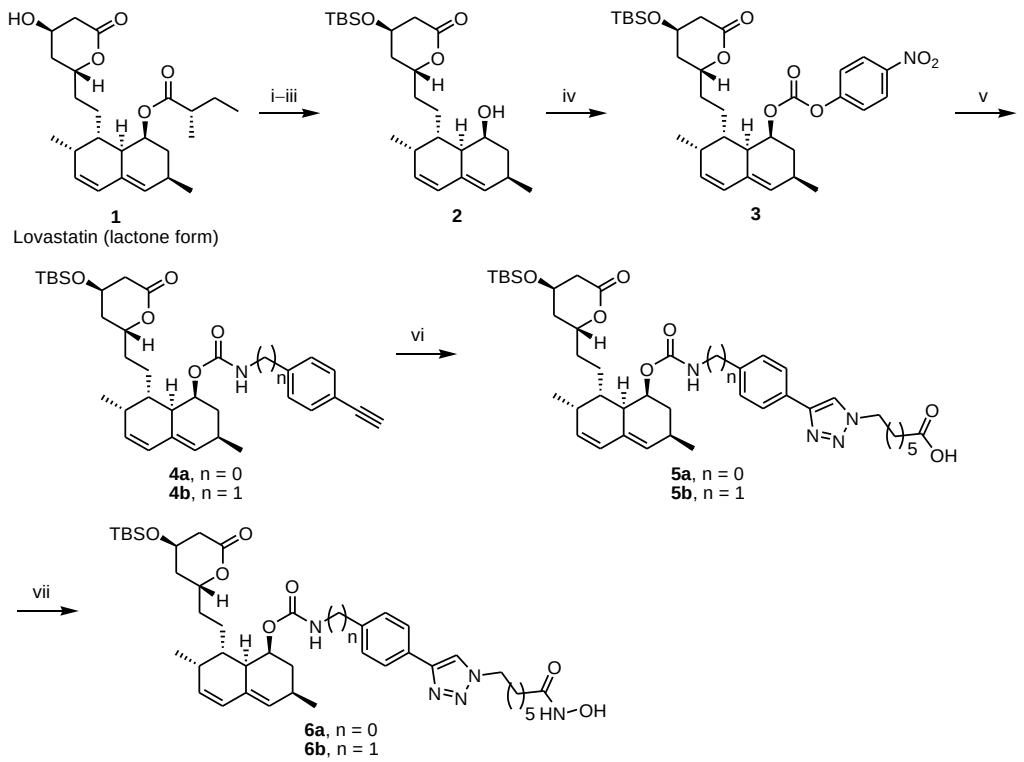

[a] Reagents and conditions: (i) KOH, H_2O/MeOH, reflux, 8 h; (ii) 6 M HCl, rt, 4.5 h; (iii) TBSCl, imidazole, CH_2Cl_2, rt, 5.5 h; 58% for 3 steps; (iv) *p*-nitrophenyl chloroformate, DMAP, pyridine, rt, 15 h; 81%; (v) 4-ethynylaniline or 4-ethynylbenzylamine, DMAP, pyridine, rt, 3–21 h; 66% for **4a**; 90% for **4b**; (vi) 7-azidoheptanoic acid, $CuSO_4 \cdot (H_2O)_5$,

sodium ascorbate, *t*-BuOH/H_2O, 60 ^oC, 18 h; (vii) $ClCO_2Et$, Et_3N, THF, 0 ^oC, 10 min; (viii) $NH_2OH \cdot HCl$, KOH, THF/MeOH, 0 ^oC, 15 min; 37% for **6a** from **4a**; 53% for **6b** from **4b**.

In another approach (Scheme 2), carbonate **3** was reacted with the allyl ester of 7-aminoheptanoic acid (**7**) to afford carbamate **8**. The allyl group in **8** was removed by the catalysis of palladium. The acid intermediate **9** was activated with ethyl chloroformate and reacted with hydroxylamine to give hydroxamate **10**.

Scheme 2. Synthesis of lovastatin derivative **10** bearing a hydroxamic acid group by merged strategy.[a]

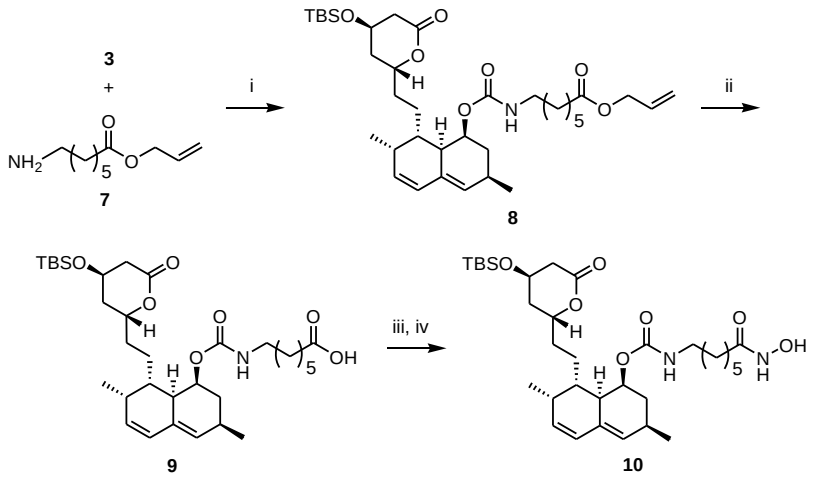

[a] Reagents and conditions: (i) DMAP, pyridine, rt, 2 h; 70%; (ii) $Pd(PPh_3)_4$, PPh_3, Et_3N, HCOOH, THF, rt, 3 h; (iii) $ClCO_2Et$, Et_3N, THF, 0 ^oC, 10 min; (iv) $NH_2OH \cdot HCl$, KOH, THF/MeOH, 0 ^oC, 15 min; 38% for **10** from **8**.

As the commercially available lovastatin is in the lactone form, we attempted to explore its direct coupling reaction with hydroxylamine to afford lovastatin hydroxamic acid (lova-HA) without involvement of tedious protection–deprotection procedures.[30] In our initial attempt, hydroxylamine was freshly prepared by neutralization of the hydrochloric salt with a base (KOH or NaOMe) in MeOH, and used as the nucleophile to react with lovastatin (**1** in the lactone form) in anhydrous THF/MeOH in the presence of Et_3N or DMAP at room temperature. Though the desired product of lova-HA (**12**) was observed by MS, ^1H and ^{13}C NMR spectral analyses, the reaction was complicated by recovery of lovastatin (in the acid form) and formation of the methyl ester. To reduce the side reactions, Lewis acid was tested to activate the lactone moiety of lovastatin while retain the nucleophilicity of hydroxylamine (method A in Scheme 3). Among the examined Lewis acids (LiCl, $MgBr_2$, $ZnCl_2$ and $CeCl_3$), using $MgBr_2$ (2 equiv) along with $NaHCO_3$ (8 equiv) for *in situ* neutralization of hydroxylamine hydrochloride (8.5 equiv) in THF/MeOH turned out to be a superior method for conversion of lovastatin (in lactone form) to **12** (79% yield). By similar procedures (method A), the lactone forms of simvastatin, atorvastatin and rosuvastatin were also successfully converted to their corresponding hydroxamic acids **13** (simva-HA), **14** (atorva-HA) and **15** (rosuva-HA) in 48%, 56% and 51% yields, respectively. The ester functionality and C=C double bonds existing in lovastatin, simvastatin and rosuvastatin were

unchanged under such mild reaction conditions of our method, whereas these functional groups might not be retained on acid-catalyzed hydrolysis or hydrogenation involved in the previously reported protection–deprotection procedures.[30] In these cases, only modest yields of the desired statin hydroxamic acids were obtained due to the competitive formation of the related methyl esters in MeOH solution. To reduce the formation of statin methyl esters in MeOH solution, we further investigated the substitution reactions of statin lactones with 50% hydroxylamine aqueous solution (method B in Scheme 3). To our satisfaction, high yields (88–95%) of statin hydroxamic acids **12**–**15** were obtained by treatment of the THF solutions of statin lactones with 50% aqueous hydroxylamine (5 equiv) for a short reaction time (1 h) at ambient temperature.

Scheme 3. Synthesis of statin hydroxamic acids **12**–**15**.

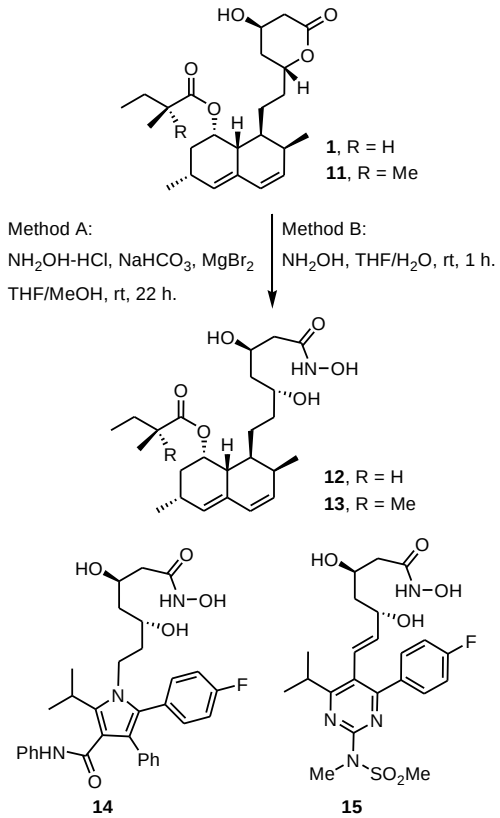

Molecular Modeling. In this work, we modeled the structures of class I HDACs (in particular HDACs 1 and 2) to focus on the design of HMGR–HDAC dual-targeting compounds for applications in cancer treatment, though inhibition of HDAC6 is reported to be a promising strategy for treatment of some neurodegenerative diseases.[31] HDAC1 and HDAC2 are homologs with high sequence identify and similarity, especially for the active site residues (Figure s1 in Supporting Information (SI)). There were no HDAC1/2 crystal structures available when we launched the design project. To simplify the design process, we mainly used the homology modeled HDAC1 as our primary protein structure of design. The

RMSD of catalytic residues between our homology modeled HDAC1 and the HDAC2 crystal structure (3MAX)[32] published in 2010 was only 0.921Å, justifying our result of homology modeling (Figure s2 in SI).

Figures 2 and 3 illustrate the predicted binding modes and the detailed protein–inhibitor interactions of compound **12** with HDAC1 and HMGR, respectively. The molecular modeling results for compounds **13**–**15** are collected in SI (Figure s3). These statin hydroxamic acids all show the 3,5,*N*-trihydroxyheptamide moiety consistently inserts into the catalytic outer-tunnel of HDAC. The hydroxamate group also chelates a zinc ion, which is important for the catalytic process of HDAC. In addition, the 3,5-dihydroxyl groups also contribute to the hydrogen-bonding interactions with the residues in the catalytic tunnel. In contrast to the previously developed HDAC inhibitors that simply contain aliphatic chains to exert hydrophobic interactions with the catalytic tunnel of HDAC, our results of molecular modeling reveal that placing polar substituents at proper locations of ligand, e.g., the OH groups at C-3 and C-5 positions in **12**, can still maintain the binding affinity to HDAC inhibitors. Thus, statin hydroxamates bearing 3,5-dihydroxyl substituents on the alkyl chain may become better HDAC inhibitors.

In another aspect, hydroxamic acid is considered as a bioisostere of carboxylic acid. Similar to the crystal structures of statin–HMGR complexes (Figure s4 in SI),[29] our molecular docking studies also indicate that the hydroxamate group in compounds **12**–**15** contributes to

substantial hydrogen bondings with at least two residues of Lys A735, Ser B684, and Lys B692 in HMGR, wherein A and B represent A and B chains of the protein. Thus, compounds **12**–**15** are also predicted to exhibit reasonable affinity to HMGR. Our alignment analysis using various binding poses of compound **12** further indicates that the binding pockets of HMGR and HDAC1 are dissimilar while the highly flexible nature of compound **12** still fits into each active site with different conformations (Figure s5 in SI).

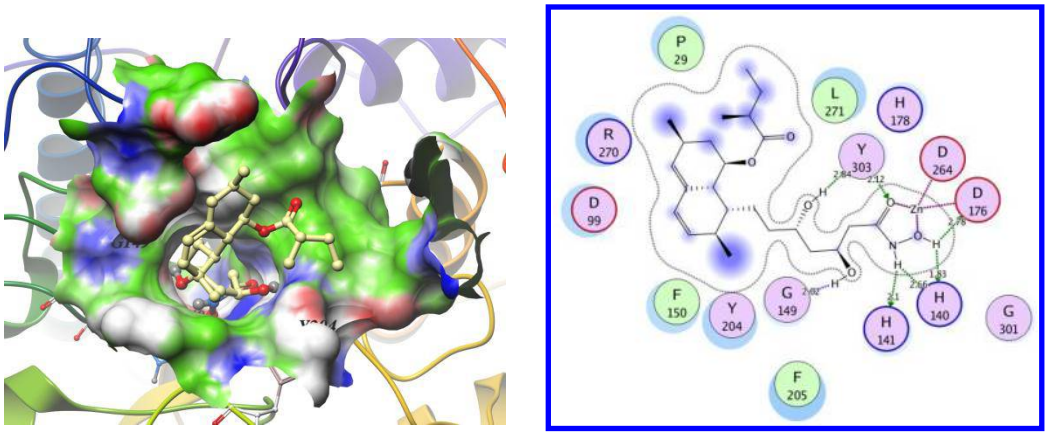

Figure 2. Predicted binding mode and receptor–ligand interaction diagrams of compound **12** on homology modeled HDAC1. The structural template, HDLP structure, was obtained from Protein Data Bank (PDB ID: 3CSR). Amino acid residues within 4.5 Å of ligand are presented in the two-dimensional interaction diagram. The blue circle on the ligand represents its exposure to the solvent. The larger circle indicates more exposure of the ligand to the solvent. The green and magenta dashed lines represent hydrogen bonding and metal chelation, respectively.

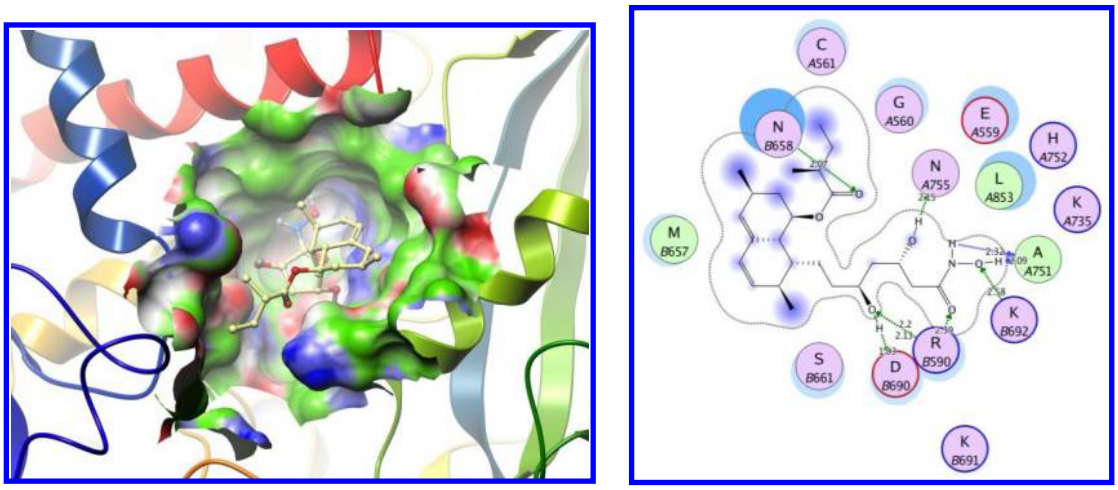

Figure 3. Predicted binding mode and receptor–ligand interaction diagrams of compound **12** on HMGR. The illustration is similar to that described in Figure 2. The letters A and B before the residue numbers represent the A and B chains, respectively, in the PDB entry of HMGR (PDB ID: 1HW9).

HMGR and HDAC Inhibition. We first used *in vitro* enzymatic assays to examine the inhibition of synthetic compounds on HMGR and HDAC activities. As shown in Table 1, compounds **6a**, **6b**, **10**, and **12–15** all inhibited HMGR activity with IC_{50} values similar to statins in nanomolar range. However, SAHA had no inhibition on HMGR activity even at a dose of 10 μM. Compounds **6a**, **6b**, **10**, and **12–15** appreciably inhibited HDAC1 (class I), HDAC2 (class I) and HDAC6 (class II) activities with IC_{50} values in nanomolar range. However, lovastatin and atorvastatin inhibited HDACs at a concentration of more than 10 μM.

These experiments clearly indicated that compounds **6a**, **6b**, **10**, and **12**–**15** acted as potent dual functional inhibitors against HMGR and HDACs.

Table 1. Inhibitory activities (IC_{50}) against HMGR and HDACs.

compound	IC_{50} (nM)[a]			
	HMGR	HDAC1	HDAC2	HDAC6
lovastatin	29.5 ± 3.5	11911 ± 681	25933 ± 651	16285 ± 1575
atorvastatin	12.9 ± 1.3	11619 ± 382	22547 ± 1618	14466 ± 567
SAHA	>10,000	20.9 ± 7.1	100.9 ± 10.0	19.4 ± 6.0
6a	36.5 ± 5.3	159.0 ± 8.4	463.3 ± 28.0	127.4 ± 21.5
6b	53.8 ± 5.2	124.7 ± 6.3	881.8 ± 9.7	34.0 ± 4.3
10	54.1 ± 2.1	122.0 ± 12.7	657.7 ± 21.1	139.7 ± 5.7
12	16.8 ± 1.9	64.8 ± 5.4	468.3 ± 27.2	51.0 ± 6.1
13	13.1 ± 1.5	63.4 ± 4.5	414.2 ± 15.5	69.5 ± 4.1
14	12.3 ± 2.7	122.9 ± 9.5	467.2 ± 19.0	86.6 ± 6.0
15	43.7 ± 1.6	125.2 ± 7.1	600.1 ± 34.0	133.3 ± 5.5

[a] Data are shown as mean ± SD of three experiments.

To further evaluate their inhibition on HMGR in lung cancer cells, compounds **6a**, **6b**, **10**,

and **12**–**15** at 1–50 μM were applied to cells for 24 h, and the HMGR activity in whole cell lysates was measured. Compounds **6a**, **6b**, **10**, and **12**–**15** effectively reduced HMGR activity in a dose-dependent manner with IC_{50} values similar to lovastatin in nanomolar range (Table 2). However, SAHA did not affect HMGR at any dose.

Table 2. Inhibition on the HMGR activity in A549 lung cancer cells.

compound	IC_{50} (μM)[a]
lovastatin	19.8 ± 2.2
SAHA	ND[b]
6a	22.3 ± 5.9
6b	16.1 ± 4.8
10	13.2 ± 5.1
12	15.9 ± 0.8
13	7.9 ± 1.4
14	5.7 ± 1.2[a]
15	14.9 ± 1.7

[a] Data are shown as mean ± SD of three experiments. [b] ND: not determined (>10 μM) due to high toxicity of SAHA to cells.

Intracellular histone acetylation status is a direct marker of class I HDAC inhibition, whereas α-tubulin is a substrate of HDAC6 (class II). As shown in Figure 4, compounds **6a**, **6b**, and **12**–**15** promoted histone and tubulin acetylations in a dose-dependent manner. SAHA and lovastatin were included for comparison.

(**A**)

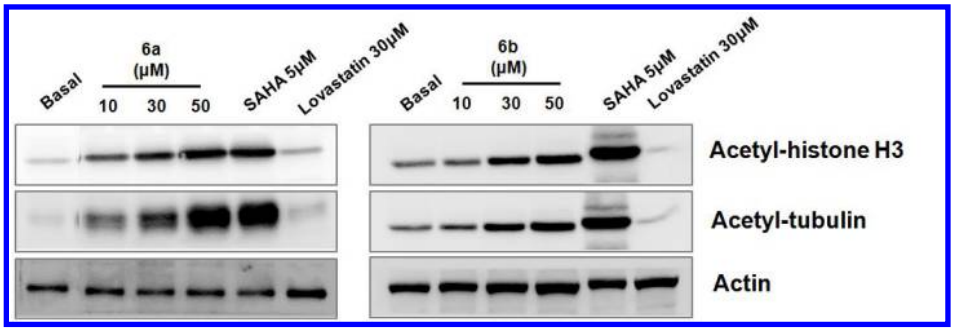

(**B**)

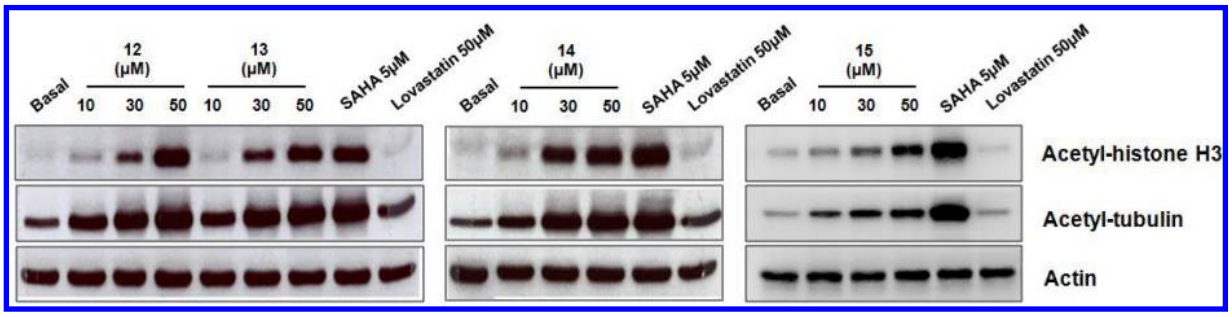

Figure 4. Effect of hydroxamate compounds on acetylation of histone H3 and tubulin in A549 lung cancer cell lines. A549 cells were treated with indicated doses of drugs for 24 h: (**A**) conjugated compounds **6a** and **6b**; (**B**) hybrid compounds **12**–**15**. SAHA (5 μM) and lovastatin (30 or 50 μM) were used for comparison. Total protein lysates were subjected to

Western blotting using antibodies specific for acetyl-histone H3, acetyl-tubulin or actin. Equivalent protein loading with similar level of β-actin was applied.

Cell Growth Inhibition. Cell viability assays were performed to determine the cytotoxicity and specificity of compounds **12**–**14** (Table 3). A549 human lung cancer cells, MEF normal mouse fibroblast cells, and HS68 normal human fibroblast cells were treated with different doses of drug for 72 h, and the IC_{50} values were evaluated. SAHA was toxic to both cancer and normal cells without specificity. The selectivity index of statins for cancer and normal cells was low. Compounds **12**–**14** significantly induced cytotoxicity in the cancer cells (IC_{50} < 20 μM), but were not toxic to the normal cells at 100 μM. Our results indicate that compounds **12**–**14** have a potential to be developed as safer drugs than statins and SAHA in cancer treatment and other therapeutic uses.

Table 3. Inhibition on the growth of cancer and normal cells.

compound	IC_{50} (μM)[a]			S.I.[b]	
	A549[a]	MEF[a]	HS68[a]	A549/MEF	A549/HS68
lovastatin	11.4 ± 6.3	35.0 ± 5.9	23.2 ± 3.5	3.1	2.0
simvastatin	16.3 ± 0.1	36.7 ± 4.4	26.4 ± 2.1	2.3	1.6
atorvastatin	8.7 ± 1.1	30.7 ± 3.2	22.7 ± 2.0	3.5	2.6

SAHA	4.5 ± 0.8	4.4 ± 1.4	4.6 ± 0.7	1.0	1.0
12	18.2 ± 3.4	> 100	> 100	> 5.6	> 5.6
13	20.0 ± 3.1	> 100	> 100	> 5.0	> 5.0
14	17.5 ± 4.7	> 100	> 100	> 5.7	> 5.7

[a] Cells were treated with indicated doses of test compounds for 72 h, and the cell viability was measured by MTT assay. Data are shown as mean ± SD of three experiments. A549: human lung cancer cells; MEF: normal mouse fibroblast cells; HS68: normal human fibroblast cells. [b] Selectivity index: the ratio of IC_{50} on cancer cell to IC_{50} on normal cell.

CONCLUSION

HDAC has been a validated target for cancer therapy. Though a potent HDAC inhibitor SAHA has been approved for treatment of cutaneous T cell lymphoma, the high toxicity of SAHA is a serious concern. In contrast, statins have shown safety and efficacy in preventing human cardiovascular diseases. The recent studies also indicate that statins may have beneficial effects in prevention and treatment of cancers. We thus conceive a new therapeutic approach for cancer treatment by concurrent inhibition of HDAC and HMGR. We have successfully synthesized a series of dual-action compounds to target HDAC and HMGR by having a hydroxamate group essential for chelation with the zinc ion in the active site of HDAC and the key structural elements of statin for binding with both proteins. In addition to

using hydroxamic acid as a surrogate of carboxylic acid, we also found that the aliphatic chains in SAHA and statin could be overlaid. Thus, the hybrid molecules **12**–**15** exhibited high inhibitory activities against both HDAC and HMGR. Our cell-based assays also showed that these statin hydroxamic acids effectively reduced the HMGR activity and promoted the acetylations of histone and tubulin in cancer cells (IC_{50} < 20 μM), but were not toxic to normal cells at the concentration as high as 100 μM.

The *in vivo* experiments, pharmacokinetics and metabolic studies of the HDAC–HMGR dual-action inhibitors are currently under investigation. Our results indicated that oral administration of compound **12** could prevent and treat azoxymethane (AOM)/dextran sulphate sodium (DSS)-induced colitis-associated colorectal cancer in mice. Treatment with compound **12** did not show any toxicity by biochemical examinations and hematoxylin and eosin (H&E) staining of various organs (manuscript in preparation). The pharmacokinetics of compound **12** has been evaluated in healthy rats through intravenous or oral administration.

We need to stress that it is still possible to find more efficient dual-action compounds by taking other possible combinations of different HMGR and HDAC inhibitors. For example, using different zinc binding groups may provide a higher affinity toward the target proteins and thus render a better therapeutic efficiency. On the other hand, changing the cap region in the dual-action compounds may achieve better selectivity to differentiate HDAC subtypes. In summary, we have demonstrated the first example of dual-action inhibitors targeting HDAC

and HMGR as a promising approach to cancer therapy.

EXPERIMENTAL SECTION

Materials and Methods. All the reagents were commercially available and used without further purification unless indicated otherwise. All solvents were anhydrous grade unless indicated otherwise. Dichloromethane was distilled from CaH_2; triethylamine was distilled from $MgSO_4$. Lovastatin and simvastatin were obtained from Lotus Pharmaceutical Company (Nantou, Taiwan). Atorvastatin was obtained from Synpac Kingdom Pharmaceutical Company (Taipei, Taiwan). SAHA was purchased from Merck (Frankfurter Sparkasse, Germany). Anti-acetylhistone H3 antibody was purchased from Millipore (Bedford, MA, USA). Anti-β-actin antibody was purchased from Gene Tex (Irvine, CA, USA). HDAC Fluorimetric Assay/Drug Discovery Kit (AK-500) was purchased from Biomol (Plymouth Meeting, PA, USA). HMG-CoA reductase activity kit (CS-1090), and anti-acetyltubulin antibody were purchased from Sigma (St. Louis, MO, USA).

All non-aqueous reactions were carried out in oven-dried glassware under a slight positive pressure of argon unless otherwise noted. Reactions were magnetically stirred and monitored by thin-layer chromatography on silica gel. Analytical thin layer chromatography (TLC) was performed on 0.25 mm silica gel 60 F_{254} plates. Compounds were visualized by UV, or using *p*-anisaldehyde, ninhydrin, phosphomolybdic acid, $KMnO_4$ or I_2 as visualizing

agent. Flash chromatography was carried out on columns packed with silica gel 60 (0.040–0.063 mm particle sizes). High-performance liquid chromatography (HPLC) was performed on Agilent 1100 Series instrument equipped with a degasser, Quat pump, and UV detector.

Melting points were recorded on an Electrothermal MEL-TEMP 1101D melting point apparatus and were not corrected. Optical rotations were measured on digital polarimeter of Japan JASCO Co. DIP-1000; $[\alpha]_D$ values are given in units of 10^{-1} deg cm^2 g^{-1}. Infrared (IR) spectra were recorded on a Nicolet Magna 550-II FT-IR spectrometer. Nuclear magnetic resonance (NMR) spectra were obtained on Varian Unity Plus-400 (400 MHz) or Bruker Avance-III 400 MHz NMR spectrometers. Chemical shifts (δ) were recorded in parts per million (ppm) relative to δ_H 7.24/ δ_C 77.0 (central line of t) for $CHCl_3/CDCl_3$ or δ_H 0.00/ δ_C 77.0 (central line of t) for TMS/$CDCl_3$, δ_H 3.31/ δ_C 49.0 for CH_3OH/CD_3OD, and δ_H 2.50 (m)/δ_C 39.5 (m) for $(CH_3)_2SO/(CD_3)_2SO$. The splitting patterns are reported as s (singlet), d (doublet), t (triplet), q (quartet), m (multiplet) and br (broad). Coupling constants (*J*) are given in hertz. The ESI–MS experiments were conducted on a Bruker Daltonics BioTOF III high-resolution mass spectrometer.

General Compound Characterization. New compounds were characterized by their physical and spectroscopic properties (mp, TLC, [α], IR, ESI–MS, ^{1}H and ^{13}C NMR). Purity of synthetic compounds **6a**, **6b**, **10**, and **12–15** was assessed to be ≥ 95% by HPLC analysis

(Agilent HP-1100) on an HC-C18 column (250 mm × 4.6 mm i.d., 5 μm particle size) using gradient elution of aqueous CH_3CN for 20–30 min at a flow rate of 1 mL/min with detection at 254 nm wavelength.

Homology Modeling. The sequence alignment between human HDAC1 and histone deacetylase-like protein (HDLP) was determined by the multiple sequence alignment between human class I HDACs (HDAC1, HDAC2, HDAC3, and HDAC8) and HDLP using the ClastalW module with BLOSUM scoring matrix in Discovery Studio 2.55 (Accelrys, Inc. San Diego, CA, USA). The homology model structure was generated and optimized by MODELLER in Discovery Studio 2.55 (Accelrys, Inc. San Diego, CA, USA). The structural template of the homology modeling of HDAC1 and HDAC2, the HDLP structure was obtained from Protein Data Bank (PDB ID: 3CSR). The one with the lowest energy score was selected as the final model.

Molecular Docking. The crystal structure of HMG-CoA reductase was taken from Protein Databank (PDB 1HW9). The structure of HDAC1 was prepared from the homology modeling described above. All non-protein molecules were deleted except the zinc ion of the HDAC complex. The receptor is prepared by AutoDock 4 suite.[33] The grid box size was adjusted to cover the original ligand and its surrounding binding pocket residues with 48 × 40 × 40 in HDAC1 and 40 × 40 × 52 in HMG-CoA reductase with grid spacing of 0.375Å. The 2D ligand structures were prepared using ChemDraw Ultra 12 and the 3D structures were

generated by OpenBabel 2.3.1.[34] The molecular docking simulations were performed by AutoDock4, with the recent reparameterized scoring function (AutoDock4^{RAP}).[35] It has been shown that the native ligand of HDAC can be reproduced with the new scoring function and a new divide-and-conquer docking approach.[36] The binding pose with lowest score in each case is selected to represent the predicted binding mode. The 3D and 2D protein–ligand interaction plots were presented using ICM Browser version 3.7-2d (Molsoft L.L.C., San Diego, USA) and Molecular Operating Environment version 2009.10 (Chemical Computing Group, Montreal, Canada), respectively.

Cell Lines and Culture Conditions. A549 human lung carcinoma cells from American Type Culture Collection (ATCC, Manassas, VA) were cultured in Dulbecco's Modified Eagle's Medium (DMEM). MEF normal mouse fibroblast cells and HS68 normal human fibroblast cells were cultured in RPMI 1640. All media were supplemented with 10% FBS, 100 U/mL penicillin G and 100 mg/mL streptomycin sulfate. Cells were maintained in a humidified incubator containing 5% CO_2 in air. Cells were subcultured by trypsinization in laminar flow when grew about 80% in the culture dishes.

HDAC Activity Assay. The HDAC activity was performed using the HDAC fluorimetric activity assay kit (BIOMOL, Plymouth Meeting, PA, USA) according to the manufacturer's instructions. Briefly, recombinant proteins of HDAC1, HDAC2 or HDAC6 were incubated with test compounds, and HDAC reaction was initiated by addition of Fluor-de-Lys substrate.

Samples were incubated for 10 min at room temperature, followed by adding developer to stop the reaction. Fluorescence was measured by fluorimetric reader with excitation at 360 nm and emission at 460 nm. The HDAC activity was expressed as arbitrary fluorescence units (AFU). The HDAC activity was calculated as a percentage of activity compared with the control group. The 50% of inhibition concentration (IC_{50}) values for the test compounds were calculated using SigmaPlot software.

HMG-CoA Reductase Activity Assay. The HMGR activity was performed using the HMGR assay kit according to the manufacturer's instructions (Sigma–Aldrich, St. Louis, MO, USA). Briefly, recombinant HMGR protein incubated with lovastatin or test compounds for 10 min at room temperature, or total cell lysate from A549 treated with lovastatin or test compounds was mixed with HMG-CoA and NADPH, and incubated for 5 min at 37 ^{o}C. The absorbance at 340 nm was measured. The 50% of inhibition concentration (IC_{50}) values for the test compounds were calculated using SigmaPlot software.

Western Blot Analysis. Following treatment with test compounds, cells were lysed on ice. Total cell lysates were prepared and subjected to SDS–PAGE using adequate percentage polyacrylamide gels. Immunoblotting was performed using specific antibodies to evaluate the expression of different proteins.

Cell Proliferation Assay. Cells were seeded at 3000 cells/well in 96-well plates and maintained for 14–16 h. Cells were treated with DMSO or various concentrations of test

compounds for 72 h, and then washed with PBS twice. A medium containing 3-(4,5-dimethylthiazol-2-yl)-2,5-diphenyl tetrazolium bromide (MTT, 0.5 mg/mL) was added, and the cells were incubated for 4 h at 37 ^{o}C under 5% CO_2. During this period, cells having functional succinate dehydrogenase in mitochondria would convert MTT to formazan. The medium was replaced with 200 μL of DMSO for 30 min at room temperature, and the 96-well plate was read by an ELISA reader at 570 nm to get the values of absorbance density. The IC_{50} values were calculated using SigmaPlot software.

General Methods for Preparation of Statin Hydroxamates. *Method A*. To a solution of lovastatin (**1**, in lactone form, 0.74 mmol) and $MgBr_2$ (1.48 mmol) in anhydrous THF/MeOH (7:3, 3 mL) was added hydroxylamine hydrochloride (6.3 mmol) and sodium bicarbonate (5.9 mmol). The mixture was stirred at ambient temperature for 22 h, and concentrated under reduced pressure. The residue was extracted with EtOAc and brine. The organic phase was dried over $MgSO_4$, filtered, concentrated, and purified by flash chromatography (silica gel, CH_2Cl_2/MeOH (15:1)) to give the desired statin hydroxamic acid.

Method B. To a solution of statin (in lactone form, 0.25 mmol) in THF (469 μL) was added 50% aqueous hydroxylamine (1.24 mmol, 76 μL). The mixture was stirred at ambient temperature for 1 h, and then concentrated under reduced pressure. The residue was purified by flash chromatography (silica gel, CH_2Cl_2/MeOH (15:1)) to give the desired statin hydroxamic acid.

(4*R*,6*R*)-6-[2-((1*S*,2*S*,6*R*,8*S*,8a*R*)-8-Hydroxy-2,6-dimethyl-1,2,6,7,8,8a-hexahydronaphthyl)ethyl]-4-*tert*-butyldimethylsilyloxy-3,4,5,6-tetrahydro-2*H*-pyran-2-one (2). Lovastatin (**1**, 9.0 g, 22.3 mmol) was heated with potassium hydroxide (12.6 g, 224.5 mmol) in H_2O/MeOH (1:6, 63 mL) at refluxing for 8 h. After adding H_2O (49.5 mL) to the mixture, MeOH was removed under reduced pressure. To the residue were added H_2O (180 mL), CH_2Cl_2 (45 mL), and 6 M HCl aqueous solution until pH = 2. The mixture was stirred at room temperature for 4.5 h, was and then neutralized with saturated $NaHCO_3$ aqueous solution. The mixture was extracted with CH_2Cl_2. The combined organic phase was dried over anhydrous $MgSO_4$, filtered and concentrated to give a deacylation product as orange oil. TLC (EtOAc) R_f = 0.33.

The crude product was treated with *tert*-butyldimethylsilyl chloride (8.7 g, 57.9 mmol) and imidazole (8.8 g, 129.1 mmol) in CH_2Cl_2 (82 mL) at room temperature for 5.5 h. The mixture was concentrated under reduced pressure, and the residue was extracted with CH_2Cl_2 and H_2O. The organic phase was dried over $MgSO_4$, filtered, concentrated, and purified by flash chromatography (silica gel, EtOAc/hexane (2:8) to EtOAc) to give the compound **2** (5.6 g, 58% overall yield from lovastatin). $C_{25}H_{42}O_4Si$; white solid, mp 141.1–142.3 ^oC; TLC (EtOAc/hexane (6:4)) R_f = 0.61; ^1H NMR ($CDCl_3$, 400 MHz) δ 5.98 (1 H, d, J = 9.6 Hz), 5.78–5.82 (1 H, m), 5.55 (1 H, br s), 4.66–4.70 (1 H, m), 4.29–4.30 (1 H, m), 4.23–4.25 (1 H, m), 2.54–2.65 (2 H, m), 2.35–2.45 (2 H, m), 2.16–2.18 (1 H, m), 1.70–1.93 (7 H, m),

1.44–1.55 (2 H, m), 1.15 (3 H, d, J = 7.6 Hz), 0.88–0.91 (12 H, m), 0.08 (6 H, d, J = 1.6 Hz); ^{13}C NMR ($CDCl_3$, 100 MHz) 170.4, 133.6, 131.3, 129.9, 128.4, 76.3, 65.1, 63.5, 39.2, 38.7, 36.8, 36.3, 35.7, 32.9, 30.7, 27.3, 25.6 (3 ×), 24.2, 23.7, 17.9, 13.9, –5.0 (2 ×).

(4*R*,6*R*)-6-(2-{(1*S*,2*S*,6*R*,8*S*,8a*R*)-8-[(*p*-Nitrophenoxy)carbonyloxy]-2,6-dimethyl-1,2,6,7,8,8a-hexahydronaphthyl}ethyl)-4-*tert*-butyldimethylsilyloxy-3,4,5,6-tetrahydro-2*H*-pyran-2-one (3). A mixture of alcohol **2** (5.0 g, 11.5 mmol), *p*-nitrophenyl chloroformate (16.2 g, 80.2 mmol) and DMAP (98.0 g, 80.2 mmol) was stirred in anhydrous pyridine (80.2 mL) at room temperature for 15 h. Pyridine was removed under reduced pressure, and the residue was extracted with CH_2Cl_2 and 1 M HCl aqueous solution. The combined organic phase was washed with saturated $NaHCO_3$ aqueous solution and brine, dried over $MgSO_4$, filtered and concentrated under reduced pressure. The residue was purified by flash chromatography (silica gel, CH_2Cl_2/hexane (6:4 to 8:2)) to give the carbonate compound **3** (5.6 g, 81%). $C_{32}H_{45}NO_8Si$; white powder, mp 146.5–147.3 ^{o}C; $[\alpha]^{25}_{D}$ = +233.9 (EtOAc, c = 1.0); TLC (EtOAc/hexane (2:8)) R_f = 0.24; IR ν_{max} (neat) 2955, 2930, 2857, 2360, 1760, 1594, 1525, 1347, 1258, 1216, 1082 cm^{-1}; ^{1}H NMR ($CDCl_3$, 400 MHz) δ 8.27 (2 H, d, J = 9.2 Hz), 7.40 (2 H, d, J = 8.8 Hz), 6.01 (1 H, d, J = 9.6 Hz), 5.79–5.83 (1 H, m), 5.57 (1 H, br s), 5.34 (1 H, br s), 4.68–4.70 (1 H, m), 4.27–4.29 (1 H, m), 2.52–2.59 (3 H, m), 2.34–2.41 (2 H, m), 2.17–2.23 (1 H, m), 1.66–2.00 (6 H, m), 1.45–1.53 (2 H, m), 1.17 (3 H, d, J = 7.6 Hz), 0.93 (3 H, d, J = 6.8 Hz), 0.86 (9 H, s), 0.06 (6 H, d, J = 5.6 Hz); ^{13}C NMR ($CDCl_3$, 100 MHz) 170.2,

155.6, 152.3, 145.3, 133.2, 131.1, 129.3, 128.1, 125.2 (2 ×), 122.0 (2 ×), 75.4, 74.5, 63.6, 39.3, 37.5, 36.7, 36.1, 32.5, 32.2, 30.8, 27.3, 25.7 (3 ×), 23.5, 22.5, 17.9, 13.9, –4.9 (2 ×); ESI–HRMS calcd. for $C_{32}H_{46}NO_8Si$: 600.2993, found: *m/z* 600.3002 $[M + H]^+$.

(4*R*,6*R*)-6-(2-{(1*S*,2*S*,6*R*,8*S*,8a*R*)-8-[(4-ethynylphenyl)carbamoyloxy]-2,6-dimethyl-1,2,6,7,8,8a-hexahydronaphthyl}ethyl)-4-*tert*-butyldimethylsilyloxy-3,4,5,6-tetrahydro-2*H*-pyran-2-one (4a). A solution of carbonate **3** (1.5 g, 2.5 mmol), 4-ethynylaniline (2.1 g, 17.6 mmol) and DMAP (2.1 g, 17.6 mmol) in anhydrous pyridine (6.3 mL) was stirred at ambient temperature for 21 h. Pyridine was removed under reduced pressure, and the residue was extracted with CH_2Cl_2 and 1 M HCl aqueous solution. The combined organic phase was washed with saturated $NaHCO_3$ aqueous solution and brine, dried over $MgSO_4$, filtered and concentrated under reduced pressure. The residue was purified by flash chromatography (silica gel, EtOAc/hexane (15:85)) to give the carbamate compound **4a** (957 mg, 66%). $C_{34}H_{47}NO_5Si$; orange oil; $[\alpha]^{25}_D$ = +213.9 (EtOAc, *c* = 1.0); TLC (EtOAc/hexane (5:5)) R_f = 0.66; IR ν_{max} (neat) 3299, 2955, 2858, 1734, 1591, 1523, 1313, 1255, 1219, 1082, 1047, 839 cm^{-1}; ^1H NMR ($CDCl_3$, 400 MHz) δ 7.41 (4 H, s), 7.00 (1 H, s), 6.00 (1 H, d, *J* = 9.6 Hz), 5.79–5.83 (1 H, m), 5.56 (1 H, br s), 5.32 (1 H, br s), 4.62–4.63 (1 H, m), 4.18–4.20 (1 H, m), 3.01 (1 H, s), 2.46–2.52 (3 H, m), 2.29–2.39 (2 H, m), 2.17–2.21 (1 H, m), 1.53–1.96 (6 H, m), 1.39–1.43 (2 H, m), 1.10 (3 H, d, *J* = 7.6 Hz), 0.91 (3 H, d, *J* = 6.8 Hz), 0.86 (9 H, s), 0.05 (6

H, d, J = 3.6 Hz); ^{13}C NMR ($CDCl_3$, 100 MHz) 170.6, 153.1, 138.8, 133.4, 132.9 (2 ×), 131.9, 129.6, 128.1, 118.0 (2 ×), 116.4, 83.5, 76.3, 75.6, 69.6, 63.5, 39.2, 37.3, 36.6, 36.3, 32.5, 32.4, 30.8, 27.4, 25.6 (3 ×), 23.4, 22.6, 17.9, 13.9, –5.0 (2 ×); ESI–HRMS (negative mode) calcd. for $C_{34}H_{46}NO_5Si$: 576.3145, found: *m/z* 576.3131 $[M – H]^-$.

(4*R*,6*R*)-6-(2-{(1*S*,2*S*,6*R*,8*S*,8a*R*)-8-[(4-Ethynylbenzyl)carbamoyloxy]-2,6-dimethyl-1,2,6,7,8,8a-hexahydronaphthyl}ethyl)-4-*tert*-butyldimethylsilyloxy-3,4,5,6-tetrahydro-2*H*-pyran-2-one (4b). A solution of carbonate **3** (500 mg, 0.8 mmol), 4-ethynylbenzylamine hydrochloride (419 mg, 2.5 mmol) and DMAP (712 mg, 5.8 mmol) in anhydrous pyridine (2 mL) was stirred at ambient temperature for 3 h. Pyridine was removed under reduced pressure, and the residue was extracted with CH_2Cl_2 and 1 M HCl aqueous solution. The combined organic phase was washed with saturated $NaHCO_3$ aqueous solution and brine, dried over $MgSO_4$, filtered and concentrated under reduced pressure. The residue was purified by flash chromatography (silica gel; EtOAc/hexane (2:8)) to give the carbamate compound **4b** (444 mg, 90%). $C_{35}H_{49}NO_5Si$; colorless oil; $[\alpha]^{25}_D$ = +217.6 (EtOAc, c = 1.0); TLC (EtOAc/hexane (5:5)) R_f = 0.57; IR ν_{max} (neat) 3306, 2955, 2829, 2857, 1727, 1509, 1461, 1359, 1259, 1081, 1044, 1016, 924, 837, 778 cm^{-1}; ^{1}H NMR ($CDCl_3$, 400 MHz) δ 7.42 (2 H, d, J = 8.0 Hz), 7.22 (2 H, d, J = 8.0 Hz), 5.97 (1 H, d, J = 9.6 Hz), 5.75–5.79 (1 H, m), 5.52 (1 H, br s), 5.31 (1 H, br s), 5.22 (1 H, br s), 4.61 (1 H, br s), 4.30–4.41 (2 H, m), 4.23 (1 H, br s), 3.05 (1 H, s), 2.54 (2 H, br s), 2.43 (1 H, br s), 2.12–2.36 (3 H, m), 1.78–1.90 (4 H, m), 1.24–1.54 (4 H, m), 1.09

(3 H, d, J = 7.2 Hz), 0.87–0.91 (12 H, m), 0.07 (6 H, d, J = 2.8 Hz); ^{13}C NMR ($CDCl_3$, 100 MHz) 170.5, 156.4, 140.0, 133.3, 132.2 (2 ×), 131.9, 129.6, 128.2, 127.2 (2 ×), 120.8, 83.3, 76.7, 75.5, 68.9, 63.6, 44.4, 39.3, 37.3, 36.5, 36.2, 32.6, 30.9, 27.4, 25.6 (3 ×), 23.2, 22.6, 17.9, 13.9, –4.9 (2 ×); ESI–HRMS calcd. for $C_{35}H_{50}NO_5Si$: 592.3458, found: *m/z* 592.3458 [M + H]$^+$.

(4*R*,6*R*)-6-(2-{(1*S*,2*S*,6*R*,8*S*,8a*R*)-8-[(4-{1-[7-(Hydroxyamino)-7-oxoheptyl]-1*H*-1,2,3-triazol-4-yl}phenyl)carbamoyloxy]-2,6-dimethyl-1,2,6,7,8,8a-hexahydronaphthyl}ethyl)-4-*tert*-butyldimethylsilyloxy-3,4,5,6-tetrahydro-2*H*-pyran-2-one (6a). A mixture of alkynyl compound **4a** (827 mg, 1.4 mmol), $CuSO_4$•$5H_2O$ (71 mg, 0.29 mmol), sodium ascorbate (168 mg, 0.85 mmol) and 7-azidoheptanoic acid **(**245 mg, 1.4 mmol) in H_2O/*t*-BuOH (1:1, 19 mL) was stirred at 60 ^{o}C for 18 h. The mixture was concentrated under reduced pressure, and the residue was extracted with EtOAc and H_2O. The organic phase was dried over $MgSO_4$, filtered, and concentrated to give a practically pure 1,3-cycloaddition product **5a**. $C_{41}H_{60}N_4O_7Si$; colorless oil; TLC (EtOAc/hexane (7:3)) R_f = 0.11.

The above-prepared carboxylic acid **5a** was treated with ethyl chloroformate (0.4 mL, 4.3 mmol) and Et_3N (0.8 mL, 5.7 mmol) in anhydrous THF (4.3 mL) at 0 ^{o}C for 10 min. A solution of hydroxylamine, freshly prepared by neutralization of hydroxylamine hydrochloride (497 mg, 7.2 mmol) with KOH (360 mg, 6.4 mmol) in anhydrous MeOH (2

mL), was added. The mixture was stirred at 0 °C for another 15 min, and concentrated under reduced pressure. The residue was extracted with EtOAc and H_2O. The organic phase was dried over $MgSO_4$, filtered, and concentrated to yield an pale orange oil, which was purified by flash chromatography (silica gel, CH_2Cl_2/MeOH (15:1 to 9:1)) to give hydroxamic acid **6a** (404 mg, 37% overall yield from **4a**). The purity of **6a** was 98% as shown by HPLC analysis on an HC-C18 column (Agilent, 4.6 × 250 mm, 5 μm), t_R = 17.9 min (gradients of 55–100% aqueous CH_3CN in 30 min). $C_{41}H_{61}N_5O_7Si$; colorless oil; $[\alpha]^{24}_D$ = +129.1 (EtOAc, *c* = 1.0); IR ν_{max} (neat) 3287, 2929, 2857, 1734, 1662, 1596, 1531, 1460, 1359, 1313, 1221, 1081, 1047, 837, 779 cm^{-1}; ^1H NMR ($CDCl_3$, 400 MHz) δ 7.73 (3 H, m), 7.50 (2 H, d, *J* = 7.2 Hz), 7.12 (1 H, br s), 6.00 (1 H, d, *J* = 9.6 Hz), 5.79–5.83 (1 H, m), 5.56 (1 H, br s), 5.33 (1 H, br s), 4.64 (1 H, br s), 4.35 (2 H, br s), 4.19 (1 H, br s), 2.30–2.50 (5 H, m), 2.12–2.20 (3 H, m), 1.26–1.96 (16 H, m), 1.11 (3 H, d, *J* = 7.6 Hz), 0.91 (3 H, d, *J* = 7.2 Hz), 0.85 (9 H, s), 0.04 (6 H, s); ^{13}C NMR ($CDCl_3$, 100 MHz) 170.8, 153.4, 147.5, 138.3, 133.5, 131.9, 129.8, 128.2, 126.4 (2 ×), 125.4, 119.2, 118.8 (2 ×), 77.2, 75.8, 69.6, 63.6, 50.0, 39.3, 37.4, 36.5, 36.4, 32.6, 32.4, 30.9, 29.8, 27.8, 27.5, 25.7 (3 ×), 25.5, 24.8, 23.4, 22.7, 17.9, 14.0, –4.9 (2 ×); ESI–HRMS calcd. for $C_{41}H_{62}N_5O_7Si$: 764.4419, found: *m/z* 764.4423 $[M + H]^+$.

(4*R*,6*R*)-6-(2-{(1*S*,2*S*,6*R*,8*S*,8a*R*)-8-[(4-{1-[7-(Hydroxyamino)-7-oxoheptyl]-1*H*-1,2,3-triazol-4-yl}benzyl)carbamoyloxy]-2,6-dimethyl-1,2,6,7,8,8a-hexahydronaphthyl}ethyl)-4-*tert*

-butyldimethylsilyloxy-3,4,5,6-tetrahydro-2*H*-pyran-2-one (6b). By a procedure similar to that for **6a**, the 1,3-dipolar cycloaddition product **5b** obtained from alkyne **4b** (734 mg, 1.2 mmol) and 7-azidoheptanoic acid (202 mg, 1.2 mmol) was activated with ethyl chloroformate and reacted with hydroxylamine (6.2 mmol) in MeOH (1.7 mL) to give hydroxamic acid **6b** (511 mg, 53% overall yield from **4b**). The purity of product **6b** was 98% as shown by HPLC analysis on an HC-C18 column (Agilent, 4.6 × 250 mm, 5 μm), t_R = 17.4 min (gradients of 55–100% aqueous CH_3CN in 30 min). $C_{42}H_{63}N_5O_7Si$; colorless oil; $[\alpha]^{23}_D$ = +171.9 (EtOAc, *c* = 1.0); IR ν_{max} (neat) 3291, 2952, 2829, 2857, 1719, 1668, 1519, 1460, 1360, 1259, 1080, 1044, 836, 778 cm^{-1}; ^1H NMR ($CDCl_3$, 400 MHz) δ 7.76 (3 H, m), 7.31 (2 H, d, *J* = 7.6 Hz), 5.98 (1 H, d, *J* = 9.6 Hz), 5.76–5.80 (1 H, m), 5.53 (1 H, br s), 5.35 (1 H, br s), 5.27 (1 H, br s), 4.59–4.61 (1 H, m), 4.30–4.47 (4 H, m), 4.17 (1 H, br s), 2.09–2.46 (8 H, m), 1.19–1.94 (16 H, m), 1.11 (3 H, d, *J* = 7.2 Hz), 0.86–0.90 (12 H, m), 0.05 (6 H, s); ^{13}C NMR ($CDCl_3$, 100 MHz) 171.0, 156.5, 147.3, 139.2, 133.3, 131.9, 129.8, 129.5, 128.2 (2 ×), 127.6, 125.8 (2 ×), 119.8, 77.2, 76.0, 68.8, 63.5, 50.1, 44.4, 39.2, 37.3, 36.5, 36.0, 32.7, 31.0, 29.8, 29.7, 27.8, 27.5, 25.7 (3 ×), 25.6, 24.8, 23.1, 22.7, 17.9, 14.0, –4.9 (2 ×); ESI–HRMS calcd. for $C_{42}H_{64}N_5O_7Si$: 778.4575, found: *m/z* 778.4584 $[M + H]^+$.

(4*R*,6*R*)-6-[2-((1*S*,2*S*,6*R*,8*S*,8a*R*)-8-{[7-(Allyloxy)-7-oxoheptyl]carbamoyloxy}-2,6-dimethyl-1,2,6,7,8,8a-hexahydronaphthyl)ethyl]-4-*tert*-butyldimethylsilyloxy-3,4,5,6-tetrahydro

-2*H*-pyran-2-one (8). By a procedure similar to that for **4a**, carbonate **3** (354 mg, 0.6 mmol) was treated with allyl 7-aminohepanoate (**7**) hydrochloric salt (393 mg, 0.78 mmol) and DMAP (505 mg, 4.1 mmol) in anhydrous pyridine (1.5 mL) at ambient temperature for 2 h to give carbamate **8** (267 mg, 70% yield). $C_{36}H_{59}NO_7Si$; colorless oil; $[\alpha]^{23}_D$ = +174.5 (EtOAc, *c* = 1.0); TLC (EtOAc/hexane (1:1)) R_f = 0.57; IR ν_{max} (neat) 3369, 2930, 2857, 1742, 1520, 1462, 1339, 1253, 1082, 926, 837, 778 cm^{-1}; ^1H NMR ($CDCl_3$, 400 MHz) δ 5.98 (1 H, d, *J* = 9.6 Hz), 5.88–5.95 (1 H, m), 5.76–5.80 (1 H, m), 5.52 (1 H, br s), 5.32 (1 H, d, *J* = 17.2 Hz), 5.23 (1 H, d, *J* = 10.4 Hz), 5.18 (1 H, br s), 4.79 (1 H, br s), 4.63–4.66 (1 H, m), 4.57 (2 H, d, *J* = 5.6 Hz), 4.28–4.29 (1 H, m), 3.20–3.23 (1 H, m), 3.05–3.10 (1 H, m), 2.56–2.63 (2 H, m), 2.09–2.42 (6 H, m), 1.26–1.88 (16 H, m), 1.08 (3 H, d, *J* = 7.2 Hz), 0.88–0.90 (12 H, m), 0.08 (6 H, s); ^{13}C NMR ($CDCl_3$, 100 MHz) 173.2, 171.5, 156.3, 133.3, 132.2, 132.0, 129.6, 128.2, 118.0, 75.8, 68.4, 64.9, 63.6, 40.7, 39.3, 37.3, 36.6, 36.3, 34.0, 32.6, 32.5, 30.9, 29.7, 28.6, 27.4, 26.2, 25.6 (3 ×), 24.7, 22.5, 17.9, 13.9, –5.0 (2 ×); ESI–HRMS calcd. for $C_{36}H_{60}NO_7Si$: 646.4139, found: *m/z* 646.4142 $[M + H]^+$.

(4*R*,6*R*)-6-[2-((1*S*,2*S*,6*R*,8*S*,8a*R*)-8-{[7-(Hydroxyamino)-7-oxoheptyl]carbamoyloxy}-2,6-dimethyl-1,2,6,7,8,8a-hexahydronaphthyl)ethyl]-4-*tert*-butyldimethylsilyloxy-3,4,5,6-tetrahydro-2*H*-pyran-2-one (10). A mixture of allyl ester **8** (268 mg, 0.4 mmol), tetrakis(triphenylphosphine)palladium (48 mg, 0.04 mmol), triphenylphosphine (22 mg, 0.08

mmol), triethylamine (0.17 mL, 1.2 mmol) and formic acid (0.047 mL, 1.2 mmol) in degassed THF (2 mL) was stirred at ambient temperature for 3 h. The mixture was concentrated under reduced pressure. CH_2Cl_2 and H_2O were added, and the mixture was acidified with 1 M HCl aqueous solution to pH = 2. The mixture was extracted with CH_2Cl_2. The combined organic phase was dried over $MgSO_4$, filtered, concentrated and separated by flash chromatography (silica gel, CH_2Cl_2/MeOH (17:1)) to give a carboxylic acid product **9** as colorless oil.

By a procedure similar to that for **6a**, the above-prepared carboxylic acid **9** was activated with ethyl chloroformate and reacted with hydroxylamine (2.1 mmol) in MeOH (0.6 mL) to give hydroxamic acid **10** (98 mg, 38% overall yield from **8**). The purity of product **10** was 97% as shown by HPLC analysis on an HC-C18 column (Agilent, 4.6 × 250 mm, 5 μm), t_R = 15.2 min (gradients of 60–100% aqueous CH_3CN in 30 min). $C_{33}H_{56}N_2O_7Si$; colorless oil; $[\alpha]^{26}_D$ = +132.2 (EtOAc, *c* = 1.0); IR ν_{max} (neat) 3288, 2929, 2857, 1713, 1522, 1462, 1359, 1255, 1081, 1046, 837, 778 cm^{-1}; ^1H NMR ($CDCl_3$, 400 MHz) δ 5.98 (1 H, d, *J* = 9.6 Hz), 5.76–5.80 (1 H, m), 5.52 (1 H, br s), 5.19 (1 H, br s), 4.88 (1 H, br s), 4.68 (1 H, br s), 4.30 (1 H, br s), 3.15–3.16 (2 H, m), 2.53–2.66 (2 H, m), 2.08–2.42 (6 H, m), 1.26–1.89 (16 H, m), 1.08 (3 H, d, *J* = 7.2 Hz), 0.89 (12 H, m), 0.08 (6 H, s); ^{13}C NMR ($CDCl_3$, 100 MHz) 171.1, 171.0, 156.5, 133.2, 131.9, 129.6, 128.2, 77.2, 68.4, 63.4, 40.5, 39.2, 37.3, 36.2, 36.1, 32.5, 32.3, 30.9, 29.5, 28.2, 27.3, 25.9, 25.6 (3 ×), 25.0, 23.0, 22.5, 17.8, 13.8, –5.0 (2 ×); ESI–HRMS calcd. for $C_{33}H_{57}N_2O_7Si$: 621.3935, found: *m/z* 621.3922 $[M + H]^+$.

(3*R*,5*R*)-7-{(1*S*,2*S*,6*R*,8*S*,8a*R*)-Hexahydro-2,6-dimethyl-8-[2-methylbutyrloxy]naphthalenyl}-3,5-dihydroxy-*N*-hydroxyheptanamide (12). Lovastatin (**1**, in lactone form) was converted to the corresponding hydroxamic acid **12** in 79% yield by general method A and 92% yield by general method B. The purity of **12** was 96% as shown by HPLC analysis on an HC-C18 column (Agilent, 4.6 × 250 mm, 5 μm), t_R = 14.1 min (gradients of 30–80% aqueous CH_3CN in 30 min). $C_{24}H_{39}NO_6$; colorless oil; $[\alpha]^{24}_D$ = +208.1 (EtOAc, *c* = 1.0); TLC (CH_2Cl_2/MeOH (9:1)) R_f = 0.32; IR ν_{max} (neat) 3323, 3017, 2963, 2932, 2872, 1725, 1659, 1459, 1382, 1264, 1191, 1115, 1081, 1016, 975, 860 cm^{-1}; ^1H NMR ($CDCl_3$, 400 MHz) δ 5.98 (1 H, d, *J* = 9.6 Hz), 5.76–5.80 (1 H, m), 5.51 (1 H, br s), 5.41 (1 H, br s), 4.27 (1 H, br s), 3.76 (1 H, br s), 2.24–2.43 (6 H, m), 1.93 (2 H, br s), 1.59–1.68 (5 H, m), 1.42–1.47 (2 H, m), 1.26 (2 H, br s), 1.06–1.11 (6 H, m), 0.87 (6 H, br s); ^{13}C NMR ($CDCl_3$, 100 MHz) 177.4, 169.7, 133.4, 131.8, 129.3, 128.1, 71.5, 68.4, 68.2, 43.0, 41.5, 40.6, 37.3, 36.6, 34.9, 32.7, 30.6, 27.4, 26.8, 24.4, 22.8, 16.2, 13.8, 11.6; ESI–HRMS (negative mode) calcd. for $C_{24}H_{38}NO_6$: 436.2699, found: *m/z* 436.2697 $[M – H]^-$.

(3*R*,5*R*)-7-{(1*S*,2*S*,6*R*,8*S*,8a*R*)-Hexahydro-2,6-dimethyl-8-[2-dimethylbutyrloxy]naphthalenyl}-3,5-dihydroxy-*N*-hydroxyheptanamide (13). Simvastatin (**11**, in lactone form) was converted to the corresponding hydroxamic acid **13** in 48% yield by general method A and

95% yield by general method B. The purity of product **13** was 98% as shown by HPLC on an HC-C18 column (Agilent, 4.6 × 250 mm, 5 μm), t_R = 20.6 min (gradients of 30–80% aqueous CH_3CN in 30 min). $C_{25}H_{41}NO_6$; colorless oil; $[\alpha]^{24}_D$ = +194.1 (EtOAc, *c* = 1.0); TLC (CH_2Cl_2/MeOH (9:1)) R_f = 0.33; IR ν_{max} (neat) 3309, 3017, 2963, 2928, 2871, 1718, 1659, 1539, 1461, 1261, 1162, 1125, 1058, 975, 860 cm^{-1}; ^1H NMR ($CDCl_3$, 400 MHz) δ 5.98 (1 H, d, *J* = 9.6 Hz), 5.76–5.79 (1 H, m), 5.49 (1 H, br s), 5.44 (1 H, br s), 4.22 (1 H, br s), 3.77 (1 H, br s), 2.22–2.44 (6 H, m), 1.99 (1 H, dd, *J* = 13.2, 8.0 Hz), 1.85–1.89 (1 H, m), 1.50–1.58 (7 H, m), 1.26 (2 H, br s), 1.09–1.12 (9 H, m), 0.80–0.87 (6 H, m); ^{13}C NMR ($CDCl_3$, 100 MHz) 178.5, 169.7, 133.2, 131.7, 129.3, 128.2, 71.4, 68.4, 68.3, 43.0, 40.6, 37.5, 36.6, 34.9, 33.0, 32.8, 30.6, 29.6, 27.2, 24.7, 24.6, 24.4, 23.0, 13.8, 9.2; ESI–HRMS (negative mode) calcd. for $C_{25}H_{40}NO_6$: 450.2856, found: *m/z* 450.2854 $[M – H]^-$.

(3*R*,5*R*)-7-[2-(4-Fluorophenyl)-5-isopropyl-3-phenyl-4-phenylcarbamoyl pyrrol-1-yl]-3,5-dihydroxy-*N*-hydroxyheptanamide (14). Atorvastatin (in lactone form) was converted to the corresponding hydroxamic acid **14** in 56% yield by general method A and 88% yield by general method B. The purity of product **14** was 95% as shown by HPLC on an HC-C18 column (Agilent, 4.6 × 250 mm, 5 μm), t_R = 14.8 min (gradients of 30–100% aqueous CH_3CN in 30 min). $C_{33}H_{36}FN_3O_5$; colorless oil; $[\alpha]^{26}_D$ = –1.3 (EtOAc, *c* = 1.0); TLC (CH_2Cl_2/MeOH (9:1)) R_f = 0.33; IR ν_{max} (neat) 3405, 3301, 3059, 2960, 2926, 1738, 1657, 1595, 1527, 1508, 1436, 1314, 1241, 1223, 1157, 1108, 1078, 1046, 843, 753, 692 cm^{-1}; ^1H

NMR (DMSO-d_6, 400 MHz) δ 10.31 (1 H, br s), 9.77 (1 H, br s), 8.68 (1 H, br s), 7.50 (2 H, d, J = 7.6 Hz), 7.18–7.24 (6 H, m), 7.07 (4 H, br s), 6.98–7.00 (2 H, m), 4.69 (1 H, br s), 4.60 (1 H, d, J = 4.0 Hz), 3.92–3.95 (1 H, m), 3.72–3.83 (2 H, m), 3.53 (1 H, br s), 3.21–3.25 (1 H, m), 2.01 (2 H, d, J = 6.0 Hz), 1.63 (1 H, br s), 1.53 (1 H, br s), 1.28–1.38 (8 H, m); ^{13}C NMR (DMSO-d_6, 100 MHz) 167.4, 166.1, 162.8, 160.3, 139.4, 135.9, 134.9, 133.4, 129.1 (2 ×), 128.7, 128.4 (2 ×), 127.6 (2 ×), 127.3, 125.3, 122.9, 120.6, 119.4 (2 ×), 117.5, 115.4, 115.2, 66.0, 65.6, 43.8, 40.9, 40.7, 25.6, 22.3 (2 ×); ESI–HRMS (negative mode) calcd. for $C_{33}H_{35}FN_3O_5$: 572.2561, found: *m/z* 572.2562 $[M – H]^-$.

(3*R*,5*S*,6*E*)-7-[4-(4-Fluorophenyl)-2-(*N*-methylmethanesulfonamido)-6-isopropyl-pyrimidin-5-yl]-3,5-dihydroxy-*N*-hydroxyhept-6-enoic amide (15). Rosuvastatin (in lactone form) was converted to the corresponding hydroxamic acid **15** in 51% yield by general method A and 95% yield by general method B. The purity of product **15** was 97% as shown by HPLC on an HC-C18 column (Agilent, 4.6 × 250 mm, 5 μm), t_R = 13.79 min (gradients of 25–80% aqueous CH_3CN in 30 min). $C_{22}H_{29}FN_4O_6S$; colorless oil; $[\alpha]^{24}_D$ = –1.1 (EtOAc, c = 1.0); TLC (CH_2Cl_2/MeOH (9:1)) R_f = 0.35; IR ν_{max} (neat) 3326, 2925, 2853, 1737, 1660, 1604, 1546, 1510, 1437, 1381, 1336, 1230, 1153, 1069, 965, 901, 845, 776 cm^{-1}; ^{1}H NMR (DMSO-d_6, 400 MHz) δ 10.32 (1 H, br s), 8.70 (1 H, br s), 7.71–7.74 (2 H, m), 7.30 (2 H, t, J = 8.8 Hz), 6.50 (1 H, dd, J = 1.2, 16.2 Hz), 5.54 (1 H, dd, J = 5.6, 16.2 Hz), 4.94 (1 H, d, J =

4.4 Hz), 4.70 (1 H, d, J = 4.8 Hz), 4.19–4.22 (1 H, m), 3.88 (1 H, br s), 3.55 (3 H, s), 3.41–3.48 (4 H, m), 2.05 (2 H, d, J = 6.4 Hz), 1.48–1.56 (1 H, m), 1.37–1.43 (1 H, m), 1.22 (6 H, d, J = 6.8 Hz); ^{13}C NMR (DMSO-d_6, 100 MHz) 174.8, 167.9, 164.3, 163.3, 161.8, 157.3, 141.7, 134.9, 134.8, 132.6, 132.5, 122.2, 121.9, 115.6, 115.4, 69.1, 65.6, 44.6, 42.0, 41.2, 33.7, 31.7, 22.0 (2 ×); ESI–HRMS calcd. for $C_{22}H_{30}FN_4O_6S$: 497.1870, found: *m/z* 497.1873 [M + H]$^+$.

ASSOCIATED CONTENT

Supporting Information Available:

Figure s1–s7, synthetic procedures, ^{1}H and ^{13}C NMR spectra of new compounds. This material is available free of charge via the Internet at http://pubs.acs.org.

AUTHOR INFORMATION

Corresponding Author

*For J.-H.L.: phone, 8862-27823212 ext. 886; fax, 8862-27823060; E-mail, jlin@ntu.edu.tw.

*For J.-M.F.: phone, 8862-33661663. fax, 8862-23637812. E-mail, jmfang@ntu.edu.tw.

Notes

The authors declare no competing financial interest.

ACKNOWLEDGEMENTS

We thank the National Science Council and Academia Sinica for financial support, as well as the National Center for High Performance Computing for computing time and facilities.

ABBREVIATIONS USED

AFU, arbitrary fluorescence units; AOM, azoxymethane; ATCC, American Type Culture Collection; atorva, atorvastatin; CVD, cardiovascular disease; DMEM, Dulbecco's Modified Eagle's Medium; DML, designed multiple ligands; DSS, dextran sulphate sodium; GGTase, geranylgeranyltransferase; H&E, hematoxylin and eosin; HAT, histone acetyltransferase; HDACi, HDAC inhibitor; HDLP, histone deacetylase-like protein; HMG, 3-hydroxy-3-methylglutaryl； HMGR, HMG-CoA reductase; HMGRi, HMGR inhibitor; HA, hydroxamic acid; lova, lovastatin; Lys, lysine; MTT, 3-(4,5-dimethylthiazol-2-yl)-2,5-diphenyl tetrazolium bromide; rosuva, rosuvastatin; SAHA, suberoylanilide hydroxamic acid; SD, standard deviation; Ser, serine; simva, simvastatin; TSA, trichostatin A.

REFERENCES

1. Kwak, E. L.; Clark, J. W.; Chabner, B. Targeted agents: the rules of combination. *Clin. Cancer Res.* **2007**, *13*, 5232–5237.
2. Sawyers, C. L. Cancer: mixing cocktails. *Nature* **2007**, *449*, 993–996.
3. Zimmermann, G. R.; Lehár, J.; Keith, C. T. Multi-target therapeutics: when the whole is greater than the sum of the parts. *Drug Discov. Today* **2007**, *12*, 34–42.
4. Keith, C. T.; Borisy, A. A.; Stockwell, B. R. Multicomponent therapeutics for networked systems. *Nat. Rev. Drug Discov.* **2005**, *4*, 71–78.
5. Jenuwein, T.; Allis, C. D. Translating the histone code. *Science* **2001**, *293*, 1074–1080.
6. Simone, C.; Peserico, A. Physical and functional HAT/HDAC interplay regulates protein acetylation balance. *J. Biomed. Biotechnol.* **2011**, *2011*, art. no. 371832.
7. Witt, O.; Deubzer, H. E.; Milde, T.; Oehme, I. HDAC family: What are the cancer relevant targets? *Cancer Lett.* **2009**, *277*, 8–21.
8. Bolden, J. E.; Peart, M. J.; Johnstone, R. W. Anticancer activities of histone deacetylase inhibitors. *Nat. Rev. Drug Discov.* **2006**, *5*, 769–784.
9. Lane, A. A.; Chabner, B. A. Histone deacetylase inhibitors in cancer therapy. *J. Clin. Oncol.* **2009**, *27*, 5459–5468.
10. Carew, J. S.; Giles, F. J.; Nawrocki, S. T. Histone deacetylase inhibitors: mechanisms of cell death and promise in combination cancer therapy. *Cancer Lett.* **2008**, *269*, 7–17.

11. Hawk, E.; Viner, J. L. Statins and cancer – beyond the "one drug, one disease" model. *N. Engl. J. Med.* **2005**, *352*, 2238–2239.

12. Minder, C. M.; Blaha, M. J.; Horne, A.; Michos, E. D.; Kaul, S.; Blumenthal, R. S. Evidence-based use of statins for primary prevention of cardiovascular disease. *Am. J. Med.* **2012**, 125, 440–446.

13. Jakobisiak, M.; Golab, J. Statins can modulate effectiveness of antitumor therapeutic modalities. *Med. Res. Rev.* **2010**, *30*, 102–135.

14. Gan, Y.; Wang, J.; Coselli, J.; Wang, X. L. Synergistic induction of apoptosis by HMG-CoA reductase inhibitor and histone deacetylases inhibitor in HeLa cells. *Biochem. Biophys. Res. Commun.* **2008**, *365*, 386–392.

15. Lin, Y.-C.; Lin, J.-H.; Chou, C.-W.; Chang, Y.-F.; Yeh, S.-H.; Chen, C.-C. Statins increase p21 through inhibition of histone deacetylase activity and release of promoter-associated HDAC1/2. *Cancer Res.* **2008**, *68*, 2375–2383.

16. Morphy, R.; Rankovic, Z. Designed multiple ligands. An emerging drug discovery paradigm. *J. Med. Chem.* **2005**, *48*, 6523–6543.

17. Frantz, S. The trouble with making combination drugs. *Nat. Rev. Drug Discov.* **2006**, *5*, 881–882.

18. Medina-Franco, J. L.; Giulianotti, M. A.; Welmaker, G. S.; Houghten, R. A. Shifting from the single to the multitarget paradigm in drug discovery. *Drug Discov. Today* **2013**,

http://dx.doi.org/10.1016/ j.drudis.2013.01.008

19. Chen, L.; Wilson, D.; Jayaram, H. N.; Pankiewicz, K. W. Dual inhibitors of inosine monophosphate dehydrogenase and histone deacetylases for cancer treatment. *J. Med. Chem.* **2007**, 50, 6685–6691.

20. Chen, L.; Petrelli, R.; Gao, G.; Wilson, D. J.; McLean, G. T.; Jayaram, H. N.; Sham, Y. Y.; Pankiewicz, K. W. Dual inhibitors of inosine monophosphate dehydrogenase and histone deacetylase based on a cinnamic hydroxamic acid core structure. *Bioorg. Med. Chem.* **2010**, *18*, 5950–5964.

21. Tavera-Mendoza, L. E.; Quach, T. D.; Dabbas, B.; Hudon, J.; Liao, X.; Palijan, A.; Gleason, J. L.; White, J. H. Incorporation of histone deacetylase inhibition into the structure of a nuclear receptor agonist. *Proc. Natl. Acad. Sci. U.S.A.* **2008**, *105*, 8250–8255.

22. Mahboobi, S.; Dove, S.; Sellmer, A.; Winkler, M.; Eichhorn, E.; Pongratz, H.; Ciossek, T.; Baer, T.; Maier, T.; Beckers, T. Design of chimeric histone deacetylase- and tyrosine kinase-inhibitors: a series of imatinib hybrides as potent inhibitors of wild-type and mutant BCR-ABL, PDGF-Rβ, and histone deacetylases. *J. Med. Chem.* **2009**, *52*, 2265–2279.

23. Cai, X.; Zhai, H.-X.; Wang, J.; Forrester, J.; Qu, H.; Yin, L.; Lai, C.-J.; Bao, R.; Qian, C. Discovery of

7-(4-(3-ethynylphenylamino)-7-methoxyquinazolin-6-yloxy)-*N*-hydroxyheptanamide (CUDc-101) as a potent multi-acting HDAC, EGFR, and HER2 inhibitor for the treatment of cancer. *J. Med. Chem.* **2010**, *53*, 2000–2009.

24. Guerrant, W.; Patil, V.; Canzoneri, J. C.; Oyelere, A. K. Dual targeting of histone deacetylase and topoisomerase II with novel bifunctional inhibitors. *J. Med. Chem.* **2012**, *55*, 1465–1477.

25. O'Boyle, N. M.; Meegan, M. J. Designed multiple ligands for cancer therapy. *Curr. Med. Chem.* **2011**, *18*, 4722–4737.

26. Morphy, R.; Kay, C.; Rankovic, Z. From magic bullets to designed multiple ligands. *Drug Discov. Today* **2004**, *9*, 641–651.

27. Chen, P. C.; Patil, V.; Guerrant, W.; Green, P.; Oyelere, A. K. Synthesis and structure–activity relationship of histone deacetylase (HDAC) inhibitors with triazole-linked cap group. *Bioorg. Med. Chem.* **2008**, 16, 4839–4853.

28. Finnin, M. S.; Donigian, J. R.; Cohen, A.; Richon, V. M.; Rifkind, R. A.; Marks, P. A.; Breslow, R.; Pavletich, N. P. Structures of a histone deacetylase homologue bound to the TSA and SAHA inhibitors. *Nature* **1999**, *401*, 188–193.

29. Istvan, E. S.; Deisenhofer, J. Structural mechanism for statin inhibition of HMG-CoA reductase. *Science* **2001**, *292*, 1160–1164.

30. Orchid Research Laboratories Ltd.: Novel hydroxamates. *Indian Patent Appl.*

1492/CHE/2007.

31. Dompierre, J. P.; Godin, J. D.; Charrin, B. C.; Cordelieres, F. P.; King, S. J.; Humbert, S.; Saudou, F. Histone deacetylase 6 inhibition compensates for the transport deficit in Huntington's disease by increasing tubulin acetylation. *J. Neurosci.* **2007**, *27*, 3571–3583.

32. Bressi, J. C.; Jennings, A. J.; Skene, R.; Wu, Y.; Melkus, R.; De Jong, R.; O'Connell, S.; Grimshaw, C. E.; Navre, M.; Gangloff, A. R. Exploration of the HDAC2 foot pocket: ynthesis and SAR of substituted *N*-(2-aminophenyl)benzamides. *Bioorg. Med. Chem. Lett.* **2010**, *20*, 3142–3145.

33. Morris, G. M.; Huey, R.; Lindstrom, W.; Sanner, M. F.; Belew, R. K.; Goodsell, D. S.; Olson, A. J. AutoDock4 and AutoDockTools4: automated docking with selective receptor flexibility. *J. Comput. Chem.* **2009**, *30*, 2785–2791.

34. O'Boyle, N. M.; Banck, M.; James, C. A.; Morley, C.; Vandermeersch, T.; Hutchison, G. R. Open Babel: an open chemical toolbox. *J. Cheminform.* **2011**, *3*, art. no. 33.

35. Wang, J.-C.; Lin, J.-H.; Chen, C.-M.; Perryman, A. L.; Olson, A. J. Robust scoring functions for protein–ligand interactions with quantum chemical charge models. *J. Chem. Inf. Model* **2011**, *51*, 2528–2537.

36. Wang, J.-C.; Chu, P.-Y.; Chen, C.-M.; Lin, J.-H. idTarget: a web server for identifying protein targets of small chemical molecules with robust scoring functions and a divide-and-conquer docking approach. *Nucleic Acids Res.* **2012**, *40*, W393–W399.

Legends of Figures, Schemes, and Tables.

Figure 1. Designed dual inhibitors for HMG-CoA reductase (HMGR) and histone deacetylase (HDAC). (**A**) Structure of a representative HMGR inhibitor. (**B**) Structures of representative HDAC inhibitors. (**C**) Design of lovastatin derivative bearing hydroxamic acid group by conjugation strategy via click reaction. (**D**) Design of lovastatin derivative bearing hydroxamic acid group by merged strategy using a short aliphatic spacer. (**E**) Design of lovastatin hydroxamic acid by fused strategy to share a common 6-carbon unit from SAHA and lovastatin. The hydroxamic acid (red) is a surrogate of the carboxylate group in lovastatin, and acts as a zinc chelation group for HDAC inhibition. The HMG-like moiety (blue) provides the appropriate interactions with HMGR and HDAC.

Figure 2. Predicted binding mode and receptor–ligand interaction diagrams of compound **12** on homology modeled HDAC1. The structural template, HDLP structure, was obtained from Protein Data Bank (PDB ID: 3CSR). Amino acid residues within 4.5 Å of ligand are presented in the two-dimensional interaction diagram. The blue circle on the ligand represents its exposure to the solvent. The larger circle indicates more exposure of the ligand to the solvent. The green and magenta dashed lines represent hydrogen bonding and metal chelation, respectively.

Figure 3. Predicted binding mode and receptor–ligand interaction diagrams of compound **12**

on HMGR. The illustration is similar to that described in Figure 2. The letters A and B before the residue numbers represent the A and B chains, respectively, in the PDB entry of HMGR (PDB ID: 1HW9).

Figure 4. Effect of hydroxamate compounds on the acetylations of histone H3 and tubulin in A549 lung cancer cells. A549 cells were treated with indicated doses of drugs for 24 h: (**A**) conjugated compounds **6a** and **6b**; (**B**) hybrid compounds **12**–**15**. SAHA (5 μM) and lovastatin (30 μM) were used as controls. Equivalent protein loading with similar level of β-actin was applied. Total protein lysates were subjected to Western blotting using antibodies specific for acetyl-histone H3, acetyl-tubulin or actin. SAHA (5 μM) and lovastatin (30 or 50 μM) were used for comparison. Total protein lysates were subjected to Western blotting using antibodies specific for acetyl-histone H3, acetyl-tubulin or actin. Equivalent protein loading with similar level of β-actin was applied.

Scheme 1. Synthesis of lovastatin derivatives **6a** and **6b** bearing hydroxamic acid group by conjugation strategy.[a]

Scheme 2. Synthesis of lovastatin derivative **10** bearing a hydroxamic acid group by merged strategy.[a]

Scheme 3. Synthesis of statin hydroxamic acids **12**–**15**.

Table 1. Inhibitory activities (IC_{50}) against HMGR and HDACs.

Table 2. Inhibition on the HMGR activity in A549 lung cancer cells.

Table 3. Inhibition on the growth of cancer and normal cells.

Table of Contents Graphic